

This article was downloaded by: [ETH Zurich]

On: 30 May 2013, At: 07:07

Publisher: Taylor & Francis

Informa Ltd Registered in England and Wales Registered Number: 1072954 Registered office: Mortimer House, 37-41 Mortimer Street, London W1T 3JH, UK



Synchrotron Radiation News

Publication details, including instructions for authors and subscription information:

<http://www.tandfonline.com/loi/gsrn20>

SLS: Pushing the Envelope Based on Stability

M. Aiba^a, P. Beaud^a, M. Böge^a, G. Ingold^a, B. Keil^a, A. Lüdeke^a, N. Milas^a, L. Rivkin^a, Á. Saá Hernández^a, T. Schilcher^a, V. Schlott^a & A. Streun^a

^a Paul Scherrer Institut, Villigen, Switzerland

Published online: 22 May 2013.

To cite this article: M. Aiba, P. Beaud, M. Böge, G. Ingold, B. Keil, A. Lüdeke, N. Milas, L. Rivkin, Á. Saá Hernández, T. Schilcher, V. Schlott & A. Streun (2013): SLS: Pushing the Envelope Based on Stability, Synchrotron Radiation News, 26:3, 4-8

To link to this article: <http://dx.doi.org/10.1080/08940886.2013.791208>

PLEASE SCROLL DOWN FOR ARTICLE

Full terms and conditions of use: <http://www.tandfonline.com/page/terms-and-conditions>

This article may be used for research, teaching, and private study purposes. Any substantial or systematic reproduction, redistribution, reselling, loan, sub-licensing, systematic supply, or distribution in any form to anyone is expressly forbidden.

The publisher does not give any warranty express or implied or make any representation that the contents will be complete or accurate or up to date. The accuracy of any instructions, formulae, and drug doses should be independently verified with primary sources. The publisher shall not be liable for any loss, actions, claims, proceedings, demand, or costs or damages whatsoever or howsoever caused arising directly or indirectly in connection with or arising out of the use of this material.

SLS: Pushing the Envelope Based on Stability

M. AIBA, P. BEAUD, M. BÖGE, G. INGOLD, B. KEIL, A. LÜDEKE, N. MILAS,
L. RIVKIN, Á. SAÁ HERNÁNDEZ, T. SCHILCHER, V. SCHLOTT, A. STREUN

Paul Scherrer Institut, Villigen, Switzerland

Introduction

The Swiss Light Source (SLS) is a synchrotron radiation user facility (2000 users/year, 18 beamlines, 5000 hrs/year) in operation at Paul Scherrer Institut (PSI) since 2001. Figure 1 presents a schematic view.

The excellent electron beam stability of $<1 \mu\text{m}$ RMS (integrated over frequencies up to 1 kHz over a time span of one week) at the radiation source points provides the basis for the high performance and efficiency of the experiments and for ambitious machine development tasks.

As the first light source of its kind, the SLS had been consequently designed for top-up operation, which is the key ingredient in beam stability by providing thermal stability of machine and beamlines and allowing the beam position monitors (BPM) to be optimized for a narrow operating range, where the highest possible resolution is realized.

In this article, we will review top-up operation at SLS and report on two major achievements based on stability, namely short pulse generation and ultra-low vertical emittance operation.

Top-up operation

Top-up operation means frequent injections to keep the stored beam current approximately constant. In SLS standard user operation, the

current is kept between 400 and 402 mA by injecting 2 mA every 2–3 minutes.

Top-up operation requires a full energy injector providing a small (low emittance) beam to minimize injection losses, sufficient acceptance of the storage ring for high capture efficiency, and reliable and economic operation of the injector chain since it is running quasi-continuously.

Experiments continue during top-up, so perturbations of the stored beam have to be kept to a minimum by careful design of the injection kickers. A gating signal is provided, so that data acquisition may pause during injection. Since photon shutters stay open during injections, radiation safety issues have to be addressed.

Injection

The booster synchrotron was a novel design optimized for top-up generation [1]: it is mounted onto the inner wall of the storage ring tunnel and has a circumference of 270 m. The lattice, built from 93 gradient dipoles, provides low emittances of 10 nm horizontal and 2 nm vertical at an extraction energy of 2.4 GeV. The large number of magnets and corresponding low bending angle per dipole results in low dispersion and thus allows the reduction of the vacuum chamber aperture and with it the magnet gaps¹ and thus the magnet power consumption: it amounts to 150 kW only in continuous operation and further reduces to 10 kW average when the booster is switched off between top-up cycles (quasi-continuous operation). The availability of the injector chain is excellent, amounting to $>99\%$ over the past 10 years of operation.

The 2.4 GeV storage ring of the SLS had been realized as a lattice of 288 m circumference, built from 12 triple bend achromats (TBA) separated by six short (4 m), three medium (7 m), and three long (11 m) dispersion-free straight sections [3]. Lattice acceptance was optimized in nonlinear optics design [4] and in machine developments [5] to provide both long beam lifetime (i.e., less frequent top-up injections) and full capture of the injected beam. A booster to ring injection efficiency close to 100% can be achieved by careful tuning.

Injection into the storage ring is done by a symmetric, trapezoidal bump formed by four dipole kickers in one long, straight section with no optical elements between, so the injection tuning is largely independent from the storage ring optics. The pulse waveforms of the four

¹This lattice concept has been further elaborated for latest low emittance light sources like MAX-IV [2], where the reduced magnet gap is exploited to increase the magnet gradients.

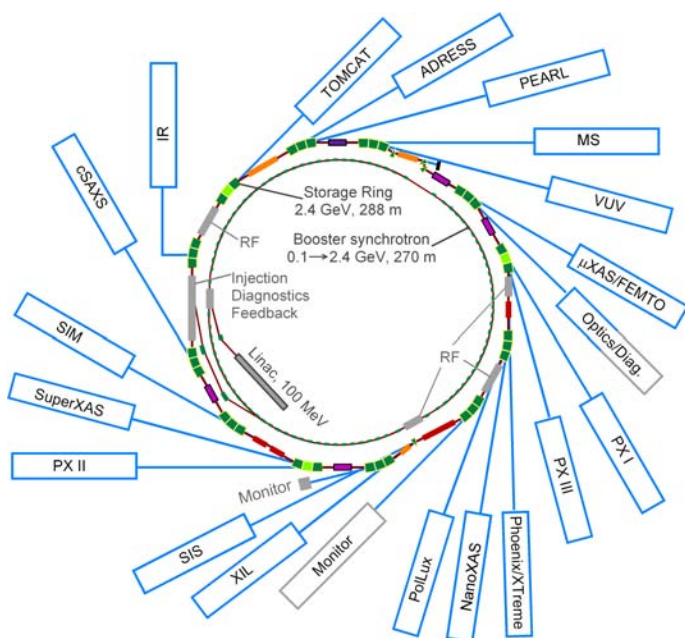


Figure 1: Schematic view of the Swiss Light Source (SLS).

kickers were carefully balanced to minimize the residual oscillation of the stored beam to about 5–15 μm in both planes at the location of the insertion devices, corresponding to beamsize fluctuations (or beam movement, respectively) of $\sim 5\%$ in the horizontal and $\sim 100\%$ in the vertical plane at the location of the radiation source points for a typical emittance coupling of 0.2%. Within about 100 turns, decoherence transforms the oscillation into a beam blow-up, which is damped down within about 20 ms.

Stability

Thermal stability is illustrated by Figure 2, showing the beam current and the distance between a BPM and an adjacent quadrupole magnet measured by the position monitoring system (POMS). During top-up operation, the thermal loads are constant and there is $<0.1 \mu\text{m}$ relative movement between the vacuum chamber and the magnets. In the case of beam loss or decaying beam, up to $\sim 10 \mu\text{m}$ are observed with time constants of ~ 40 minutes. A larger time constant of ~ 100 minutes is observed for beamline components [6]. Reproducibility (after beam loss and refill and reaching thermal equilibrium again) is better than $1 \mu\text{m}$.

The SLS storage ring is equipped with a digital BPM system [7] with six gain ranges for operation at different beam currents. Since the current is almost constant during top-up operation, the BPMs were thoroughly optimized at the lowest gain (highest current) range to provide a resolution of 130 nm for frequencies $<95 \text{ Hz}$ [6]. The relative orbit corrector power supply precision is $\sim 10^{-6}$ and the reproducibility is $\sim 10^{-5}$. The reproducibility of the corrector field is $\sim 1 \mu\text{rad}$ due to hysteresis effects; however, this is not relevant since the BPMs are used to determine the corrector setting in the orbit feedback loop. BPM offsets

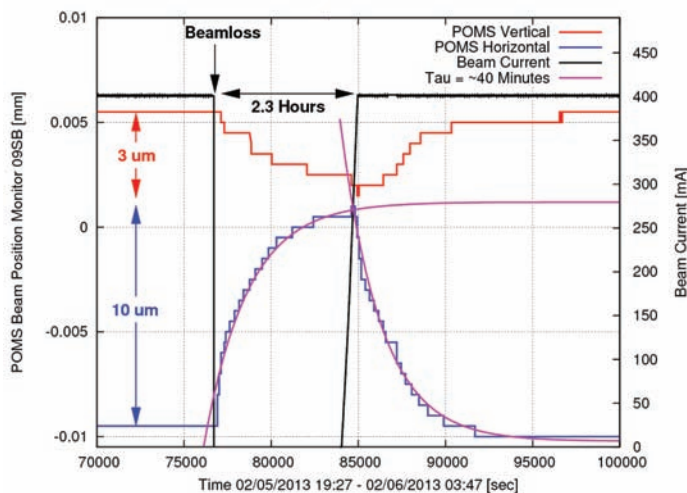


Figure 2: Position monitoring system (POMS) readings of the relative distance between a BPM and the adjacent quadrupole magnet (red, blue) and beam current (black) recorded during a beam loss event. Changes of beam current result in relative movements between BPM blocks and adjacent magnets at a time constant of about 40 minutes.

ACHIEVE HIGHEST VACUUM PERFORMANCE

Agilent TwisTorr 304 FS

The new generation Agilent 300 l/s turbo pump with Agilent Floating Suspension

- HIGH PERFORMANCE: Proven best performance on the market, with New TwisTorr stages optimized for H_2 Compression Ratio
- INNOVATION: Agilent Floating Suspension, the breakthrough bearing technology that reduces acoustical noise and vibration
- RELIABILITY: Ideal for demanding instrumentation, academic and research applications

Learn more:

www.agilent.com/chem/TwisTorr304FS

Toll Free Number for United States:

1 800 882 7426

Toll Free Number for Europe:

00 800 234 234 00

The Measure of Confidence

Learn more:

www.agilent.com/chem/TwisTorr304FS

© Agilent Technologies, Inc. 2013



Agilent Technologies



TECHNICAL REPORTS

relative to adjacent quadrupoles are regularly measured by the so-called beam-based alignment (BBA) method with a precision of $2.5\ \mu\text{m}$ and reproducibility (after one day) of $5\ \mu\text{m}$ [8]. The zero readings of the BPMs are re-calibrated with the measured offsets after every shutdown. Variations are within $\pm 50\ \mu\text{m}$.

A fast orbit feedback system (FOFB) [9] attenuates orbit distortions at a sampling rate of 4 kHz by a factor ~ 100 at 2 Hz, reaching unity gain at ~ 95 Hz, and thus efficiently suppresses low frequency orbit distortions originating from opening and closing of the insertion devices. The FOFB is capable of operating with an arbitrary reference electron orbit. Thus occasional requests from the beamlines to vary photon beam position and angle can be included. The POLLUX [27] and PEARL [28] beamlines at SLS switch polarization of synchrotron radiation by driving vertical angular bumps of $300\ \mu\text{rad}$ at a rate of up to 1 Hz. These significant orbit manipulations also stay invisible for all other beamlines in terms of transverse coupling thanks to a feed-forward compensation scheme utilizing dedicated skew quadrupoles [10].

The distortion of the electron orbit due to a gap change of an undulator is corrected by the FOFB, thus preventing any variation of the orbit at the source points of the other beamlines; i.e., the FOFB decouples the beamlines. However, this does not cover distortions inside the undulator, where the gap was changed, resulting in a missteering of the photon beam. Since this effect is reproducible, local correctors at the undulators are set based on fine-tuned feed-forward tables, which have been established from dedicated local electron BPMs and beamline photon BPMs [11]. Furthermore, photon BPM readings are utilized to manipulate electron BPM references within the FOFB loop in order to stabilize the photon beam; however, at a rather low rate of 0.5 Hz. By these means, a photon beam stability of $\sim 1\ \mu\text{m}$ RMS up to 100 Hz was achieved at the photon BPMs [12].

Safety issues

The problem of radiation safety in top-up operation was approached in a pragmatic way by simply monitoring radiation levels during operation, and up to now no increase above the allowed limits has been observed in areas accessible during operation.

Due to missteering or coupling, injection losses mainly occur at locations of low vertical aperture. In order to protect low gap undulators, an impedance-optimized movable collimator was installed in the injection region to define the minimum aperture and to localize losses in the best shielded section of the tunnel.

The laser beam slicing insertion FEMTO

Very short, intense pulses of light have the ability to excite matter far from equilibrium on extremely short time scales. The subsequent real-time dynamics have the potential to reveal the subtle interplay of forces that ultimately determines the properties of materials. Femtosecond laser-pump/X-ray-probe methods have proven to be a highly versatile tool by procuring direct access to the transient atomic and electronic structure. Two classes of experiments are performed at FEMTO: time-resolved X-ray diffraction (trXRD) and X-ray absorption (trXAS)

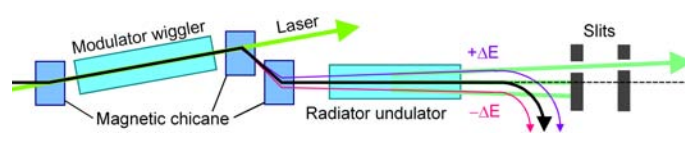


Figure 3: Schematic layout of the FEMTO insertion.

experiments. In crystalline systems trXRD provides information about coherent transient changes of long-range order, whereas trXAS as a complementary technique measures local electronic and structural changes. In both cases a typical measurement allows the reconstruction of atomic distances with a precision of $<0.01\ \text{\AA}$.

FEMTO at SLS is the first and currently only storage-ring-based undulator source providing tunable, hard X-ray (4.5–12 keV) sub-picosecond pulses [13]. As schematically shown in Figure 3, it consists of a modulator wiggler, where a high-power 50 fs FWHM laser resonantly modulates the energy of electrons in a thin slice of the bunch, a subsequent magnetic chicane translating the energy modulation into a horizontal displacement, and an in-vacuum undulator emitting the hard X-ray radiation. Collimators in the beamline extract the radiation from the modulated electrons.

The FEMTO installation had some side-effects on the storage ring: the chicane increased the emittance from 5.0 to 5.5 nm and increased the ring circumference, which required a shift of the radio frequency and retuning of the cavities. The breaking of ring periodicity was mitigated by restoring the betatron phase advances over the FEMTO straight and feed-forward tables as function of modulator gap was implemented. When the modulator is closed, the emittance increases to 6.8 nm. A local feed-forward correction of storage ring tunes compensates the perturbation of ring periodicity due to the wiggler focusing [11].

The beamline optics and collimators are adjusted to only accept the phase space of the pulsed photons and largely suppress radiation from the core beam and from adjacent bending magnets. However, the laser repetition time is much shorter than the damping times of the ring, so the modulated electrons from previous slicings will form a halo around the electron bunch. Parts of this halo cover the same phase space as the new pulse and thus generate a background to the experiment, which increases with the laser repetition rate that is currently set to 2 kHz. Depending on the bandwidth used, the halo to sliced pulse ratio is typically in the range from 5 to 15%.

Routinely, X-ray pulses of ~ 150 fs duration are achieved with a maximum flux of $4 \cdot 10^5$ photons/sec/0.1%BW at 5 keV. This flux is low compared to that generated at an X-ray free electron laser and has to be compensated by a longer time of measurement, which is affordable since laser slicing operates as an “add on” of the existing storage ring and interferes little with other experiments.

To study the dynamics of long-range order in solid materials, initial experiments at FEMTO focused on developing suitable trXRD techniques and on understanding fundamental aspects of electron-phonon interactions in model systems where the unit cell contains only two or three atoms [14]. More recently, these techniques were applied to more

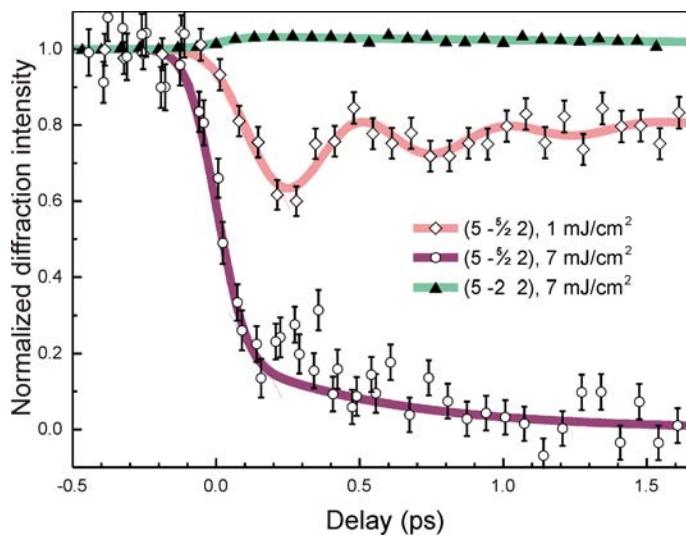


Figure 4: Time-resolved XRD data obtained measuring a very weak (~ 1 ph/s) superlattice Bragg reflection on a charge and orbitally ordered manganite [15]. (\diamond) At low excitation fluence laser-induced partial melting of the charge and orbital order launches the ultrafast displacement of a subset of the atoms within the unit cell. The initially coherent oscillation of these atoms about their new equilibrium coordinates is clearly observed. (\circ) At high fluence the superlattice peak disappears on a sub-picosecond time scale, demonstrating the ultrafast change of structural symmetry accompanying this insulator-to-metal phase transition. (\blacktriangle) The measurement on the regular (5 - 2 2) Bragg peak establishes the integrity of the crystal lattice in the course of this experiment.

complex materials, in particular focusing on the structural dynamics related to laser-induced phase transitions [15, 16]. The element specificity of trXAS has been applied to address electronic and structural dynamics related to the magnetization of metal–ligand complexes [17] and to probe the changes of the solvent shell structure upon electron abstraction of aqueous iodide [18]. Despite the low photon flux, these experiments were successful because of the exceptional stability of the SLS storage ring and the intrinsic synchronization of pump and probe pulses that allow the acquisition of very weak signals over several days (see Figure 4).

The energy modulation in FEMTO translates into a temporal modulation of the bunch current due to time of flight effects in the dipole magnets of the chicane and the storage ring arcs, and the resulting temporal structure emits coherent synchrotron radiation (CSR) in the THz range. Standard measurements of THz intensity using InSb bolometers are performed for tuning FEMTO (i.e., optimizing and monitoring the overlap of laser and electron beam). Detailed measurements were performed using electro-optical sampling techniques using a GaP crystal and revealed that CSR acts back on the electron distribution leading to a retarded dilution of the modulation [19].

THz radiation was also recorded in almost isochronous lattice optics for providing 50 mA stored beam of 10 ps FWHM pulses and compared to streak camera measurements [20].

Ultra low vertical emittance²

Efforts to reduce the vertical emittance to values below the diffraction limit (i.e., below ~ 10 pm) seem undesirable from the synchrotron radiation users' point of view, and thus are driven mainly by the particle physics community in the context of particle factory and linear collider damping ring developments.

However, in a light source, beam lifetime (and with it top-up frequency) is usually dominated by intrabeam (Touschek) scattering, leading to a longitudinal momentum change of particles. These particles will follow dispersive orbits and, if the scattering occurred in a dispersive region of the lattice, also execute oscillations around these orbits. If the lattice contains substantial coupling between horizontal and vertical planes, particles may get lost at small vertical apertures as they are imposed by the narrow gaps of the short-period undulators operated to provide hard X-rays. The same happens with the injected beam, which oscillates around the stored beam, in top-up operation, when the undulator gaps remain closed.

Magnet misalignments like roll errors, transverse displacements and, in particular, steps between adjacent magnet girders are sources of vertical dispersion and transverse coupling, which both increase the vertical equilibrium emittance. While coupling should be as small as possible, vertical dispersion may be excited on purpose to blow up vertical emittance in order to gain lifetime, since the Touschek scattering rate scales linearly with the bunch density [21]. In order to establish coupling control, however, minimization of vertical emittance is an obvious goal. Therefore PSI, CERN, INFN-LNF and MAX-IV Lab established the work package “SLS Vertical Emittance Tuning” (SVET) in the EU FP7 collaboration TIARA [22]. The main objectives of SVET are to build a high-resolution beam size monitor, to establish methods for coupling control, and to study intrabeam scattering experimentally.

Measurements of vertical dispersion and coupling are based on differences between orbit measurements for different beam momentum (i.e., radio frequency) and for different orbit corrector excitations (i.e., orbit response matrix measurements). Stability of the orbit over the time of a measurement of the order of minutes is an indispensable prerequisite for a precise result. In 400 mA top-up operation vertical dispersion could be measured at a precision of ~ 50 μm and was suppressed down to 1.25 mm RMS using 12 dispersive skew quadrupoles. Main response matrix coefficients are measured with a reproducibility of $\sim 1\%$. However, the corresponding coupling coefficients describing the crosstalk of motion in the horizontal and vertical plane are a factor of ~ 50 smaller for well-corrected transverse coupling and thus very close to the reproducibility level of successive response matrix measurements.

Several methods have been applied [23]: first, the roll errors of the BPMs were determined to exclude fake vertical orbit readings. To remove a major source of vertical dispersion, the remotely movable girders of the storage ring [29] were aligned vertically at 400 mA stored

²The research leading to these results has received funding from the European Commission under the FP7-INFRASTRUCTURES-2010-1/INFRA-2010-2.2.11 project TIARA (CNI-PP). Grant agreement no 261905.

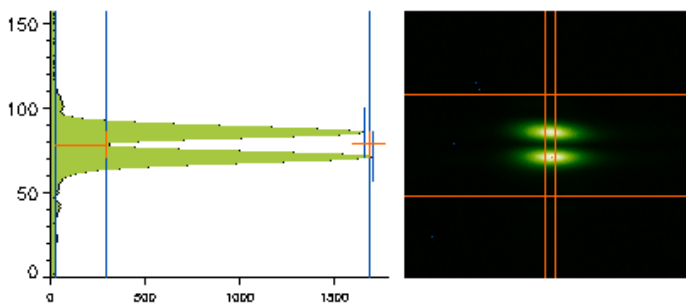


Figure 5: Image of vertical polarized near-UV (364 nm) synchrotron light. Information on beam size is contained in the peak-to-valley ratio of the beam profile.

beam with running FOFB in order to confirm success by observing the reduction of the corrector strengths in the vicinity of the girders being moved. Then corrections of vertical dispersion and transverse coupling were iterated until the procedure saturated due to orbit measurement errors/reproducibility and model deficiencies. Finally, a model independent random optimization procedure was applied which empirically tried all non-dispersive skew quadrupoles in order to minimize the beam size as observed at an already existing beam size monitor. It eventually saturated when the resolution of the monitor was reached and then was stopped at an extremely low vertical emittance value of 0.9 ± 0.4 pm. This is only five times larger than the natural quantum limit given by direct photon recoil.

The beam size monitor in operation at SLS is based on imaging the beam in vertical polarized visible or near UV light (see Figure 5): since the upper and lower lobes are of opposite vertical polarization, light is extinguished in the midplane of the image for an ideal beam of zero vertical beam size. Finite beam size, however, will result in non-zero midplane intensity and thus can be obtained from a calibration table established from simulation data. Finally, vertical emittance is inferred using the measured optical functions [24].

A second, new monitor based on the same principle was developed in order to extend the range of beam size measurements down to ~ 2 μm , corresponding to a vertical emittance of ~ 0.3 pm in the SLS lattice. Unlike the old monitor, which is located inside the tunnel, the new one is like a small beamline, ending in a hutch outside the tunnel in order to get larger magnification and to ease maintenance and operation. The refractive optics (lens) is replaced by a reflective optics (toroid) to have wavelength-independent focusing and to avoid UV-induced degradation of the silica lens observed at the old monitor [25].

Synchrotron radiation users profit from coupling suppression since it enables further reduction of undulator gaps and periods in order to increase the photon energy. This process has already been started with the successful operation of a cryogenic permanent magnet undulator (CPMU) of 14 mm period, 1.68 m length, and a minimum full gap of 3.5 mm to deliver X-rays up to 40 keV for materials research [26].

Summary and outlook

Beam stability was the crucial issue in design, commissioning, operation, and upgrade of the Swiss Light Source. Based on concepts innovative at that time, like top-up injection, digital BPM systems, fast orbit feedback, and digital power supplies, and after implementation of various methods for orbit stabilization and compensation of lattice imperfections and optics distortions, a photon beam stability of < 1 μm RMS at the beamline front ends was achieved. This level of stability in conjunction with a 98% availability of the SLS not only provided to date a decade of excellent working conditions for synchrotron radiation users, but also established a base for ambitious machine developments like short pulse generation by laser slicing and ultra-low vertical emittance tuning, which are relevant for future accelerator projects as well.

The next steps will be commissioning of the new beam size monitor in 2013 and a full upgrade and significant performance increase of the BPM system electronics based on the PSI-developed E-XFEL/Swiss-FEL platform until 2016. ■

References

1. A. Streun et al., *Nucl. Instrum. Meth. A* **562**, 1 (2006).
2. M. Eriksson et al., *Nucl. Instrum. Meth.* **587**, 221 (2008).
3. M. Böge, *Proc. EPAC-2002*, 39 (2002).
4. L. Rivkin et al., *Nucl. Instrum. Meth. A* **404**, 237 (1998).
5. M. Böge et al., *Proc. PAC-09*, 2282 (2009).
6. M. Böge et al., *Proc. PAC-05*, 1538 (2005).
7. V. Schlott et al., *Proc. DIPAC-99*, 168 (1999).
8. M. Böge et al., *Proc. EPAC-2002*, 1127 (2002).
9. T. Schilcher et al., *Proc. EPAC-2004*, 2523 (2004).
10. M. Böge et al., *Proc. EPAC-2006*, 3610 (2006).
11. J. Chrin et al., *Nucl. Instrum. Meth. A* **592**, 141 (2008).
12. T. Schilcher et al., *Proc. DIPAC-2005*, 273 (2005).
13. G. Ingold et al., *Sync. Rad. News* **20**(5), 35 (2007); P. Beaud et al., *Phys. Rev. Lett.* **99**, 174801 (2007).
14. S. L. Johnson et al., *Phys. Rev. Lett.* **100**, 155501 (2008); S. L. Johnson et al., *Phys. Rev. Lett.* **102**, 175503 (2009); S. L. Johnson et al., *Phys. Rev. Lett.* **103**, 205501 (2009).
15. P. Beaud et al., *Phys. Rev. Lett.* **103**, 155702 (2009).
16. E. Möhr-Vorobeva et al., *Phys. Rev. Lett.* **107**, 036403 (2011); S. O. Mariani et al., *Phys. Rev. Lett.* **108**, 087201 (2012).
17. C. Bressler et al., *Science* **323**, 489–492 (2009).
18. V.-T. Pham et al., *J. Am. Chem. Soc.* **133**, 12740–12748 (2011).
19. F. Müller et al., *Phys. Rev. ST-AB* **15**, 070701 (2012).
20. N. P. Abreu et al., *Proc. PAC-09*, 2285 (2009).
21. C. Steier et al., *Proc. PAC-03*, 3213 (2003).
22. Test Infrastructure and Accelerator Research Area (TIARA), www.eu-tiara.eu.
23. M. Aiba et al., *Nucl. Instrum. Meth. A* **694**, 133 (2012).
24. Å. Andersson et al., *Nucl. Instrum. Meth. A* **591**, 437 (2008).
25. N. Milas et al., TIARA-REP-WP6-2012-015 (2012).
26. P. R. Wilmott et al., submitted to *J. Sync. Rad.* (2013).
27. J. Raabe et al., *Rev. Sci. Instrum.* **79**, 11 (2008).
28. P. Oberta et al., *Nucl. Instrum. Meth. A* **635**, 116 (2011).
29. S. Zelenika et al., *Nucl. Instrum. Meth. A* **467**, 99 (2001).